Applied Clay Science 95 (2014) 275–283

Contents lists available at ScienceDirect

Applied Clay Science

journal homepage: www.elsevier.com/locate/clay

Research paper

Catalytic wet peroxide oxidation of 4-chlorophenol over Al-Fe-, Al-Cu-, and Al-Fe-Cu-pillared clays: Sensitivity, kinetics and mechanism

Shiwei Zhou [a,b], Changbo Zhang [c], Xuefeng Hu [b], Yuehua Wang [c], Rui Xu [b], Chuanhai Xia [b], Hua Zhang [b], Zhengguo Song [c,*]

[a] Key Laboratory of Soil Environment and Pollution Remediation, Institute of Soil Science, Chinese Academy of Sciences, Nanjing 210008, China
[b] Key Laboratory of Coastal Zone Environmental Processes and Ecological Remediation, Yantai Institute of Coastal Zone Research, Chinese Academy of Sciences, Yantai 264003, China
[c] Agro-Environmental Protection Institute, Ministry of Agriculture, Tianjin 300191, China

ARTICLE INFO

Article history:
Received 8 October 2013
Received in revised form 17 April 2014
Accepted 22 April 2014
Available online 19 May 2014

Keywords:
Fe Cu-Pillared clays
Thermal structural evolution
4-Chlorophenol
Peroxide oxidation
Surface-catalyzed decomposition

ABSTRACT

Al-Fe-, Al-Cu-, and Al-Fe-Cu-PILCs were synthesized, characterized and tested in the catalytic wet peroxide oxidation of 4-chlorophenol (4-CP). An apparent induction period followed by a rapid oxidation was observed during the Fenton-like reaction, and the whole reaction could be modeled well using a Fermi's kinetic equation ($R^2 = 0.9938 \sim 0.9993$). The generation of hydroxyl radicals ($HO^{\bullet}$) from surface-catalyzed decomposition of H_2O_2 was the oxidation cause whereas the dissolution of active metals was its result. Accordingly, induction period was the cause of heterogeneous surface activation (catalysis or modification) for more $HO^{\bullet}$ formed by decreasing pH. 4-CP oxidation proceeded via 4-chlorocatechol (major) and hydroquinone (minor) pathways, along the formation of main intermediate (5-chloro-1,2,4-benzentriol). Finally besides CO_2, H_2O and Cl^- two main compounds (I and II) formed, where the former was identified as 2,4-dioxopentanedioic acid whereas the latter as ferric-oxalate complex. There were marked structural and active differences between Al-Fe-PILC and Al-Cu-PILC in which compared to the latter, the former possessed higher SSA and activity but its optimal calcination temperature was lower and the induction time was also longer. In addition, compound II accounted for a considerable proportion in Al-Fe-PILC system whereas compound I was almost only component in Al-Cu-PILC system.

1. Introduction

Catalytic wet peroxide oxidation (CWPO) has been reported to be one of the most promising technologies for the removal of toxic organic compounds in wastewaters, because it could deplete nearly completely a wide range of non-biodegradable pollutants under very mild conditions of atmospheric pressure and room temperature (Garrido-Ramírez et al., 2010; Liotta et al., 2009; Perathoner and Centi, 2005; Rokhina and Virkutyte, 2011). During CWPO reaction, to enhance the decomposition of H_2O_2 to hydroxyl radicals ($HO^{\bullet}$) which were traditionally thought to be active species responsible for the destruction of pollutants, the development of active and stable catalysts was highly desirable. Recently, clays pillared with aluminum and iron or copper (designated Al-Fe-PILC or Al-Cu-PILC) have been widely used to catalyze the degradation of phenolic substrates in view of their outstanding advantages such as inexpensiveness and wide availability, no or marginal leaching of active metal ions and wide range of pH operations (Garrido-Ramírez et al., 2010; Gil et al., 2010; Liotta et al., 2009; Perathoner and Centi, 2005).

It was generally accepted that compared to Cu, Fe was easier to take part in the Al pillar, decorating the pillar or isomorphic substitution (Barrault et al., 1998; Galeano et al., 2010; Guélou et al., 2003). Therefore, there were fine structural and corresponding catalytic differences between Al-Fe-PILC and Al-Cu-PILC. For example, Caudo et al. (2007) evidenced that Al-Cu-PILC showed a lower formation of oxalic acid (main reaction intermediate) with respect to Al-Fe-PILC in the CWPO of phenolic compounds, and Al-Fe-PILC showed a slightly better rate of attack on the aromatic ring in the phenolic compounds. Additionally, Marinkovic-Neducin et al. (2004) showed that the fine changes in interlayer surrounding and porous/microporous structure with calcination temperature (≤600 °C) occurred, which depended on the nature of the second pillaring ion (Fe or Cu). This implied that there existed different structural sensitivity with increasing calcination temperature for the two types of PILCs. However, not enough work on the structural and reactive evolvements of PILCs under heating has been performed (Marinkovic-Neducin et al., 2004; Sanabria et al., 2010; Vicente et al., 2001), so that the applied catalysts during wastewater treatment were calcined optionally under different temperatures, like 300 °C (Mojović et al., 2009), 400 °C (Kim and Lee, 2004), 500 °C (Caudo et al., 2008; Galeano et al., 2010) for Al-Cu-PILCs, respectively.

Chlorophenols (CPs) were ubiquitous in wastewater of various industries, such as manufactures of preservatives, pesticides and dyes, and pulp and paper industries. Due to the high toxicity and hard biodegradability, most of them have been listed as priority pollutants, and the

* Corresponding author. Tel./fax: +86 22 23613820.
E-mail address: forestman1218@163.com (Z. Song).

http://dx.doi.org/10.1016/j.clay.2014.04.024
0169-1317/

limiting permissible concentration in drinking water should not exceed 10 μg L^{-1} (Pera-Titus et al., 2004). So, the development of efficient methods for CP removal was becoming an important field of study. In the last few years, the CWPO technology for the abatement of CP-bearing wastewater using Al-Fe- and Al-Cu-PILCs at room temperature and atmospheric pressure has been shown to be successful (Catrinescu et al., 2011, 2012; Khanikar and Bhattacharyya, 2013; Khankhasaeva et al., 2008; Molina et al., 2010; Zhou et al., 2011a). However, there were still significant knowledge gaps on understanding the kinetic process and interaction mechanism of this complicated Fenton-like reaction. Little information in literature was available and somewhat conflictive. For example, some researchers considered the dissolution of a portion of iron ions for the homogeneous Fenton reaction to take place (Belaroui and Bengueddach, 2012); others evidenced CPs reacted $HO^{\bullet}$ produced mainly by surface-catalyzed decomposition of H_2O_2 (Khankhasaeva et al., 2008; Molina et al., 2010); Catrinescu et al. (2011, 2012) showed the presence of two iron species in Al-Fe-PILCs: low-nuclearity ferric oxides and well-ordered hematite-like nanoparticles, and the former seemed to be responsible for the iron leaching and for the differences in the catalytic activity. Further, they suggested a combined heterogeneous-homogeneous mechanism could be envisaged for the reaction system.

This article presented our research on the structural and catalytic sensitivity of Al-Fe-, Al-Cu-, and Al-Fe-Cu-PILCs, and on the kinetics and mechanism of oxidation of 4-chlorophenol (4-CP) during CWPO reaction. In this study, we attempted to clarify the surface-catalyzed oxidation mechanism through investigating the structural and active differences between Al-Fe-PILC and Al-Cu-PILC, the cause of induction period, the release kinetics of Cl^- and metal ions (Fe and/or Cu), the generation process of $HO^{\bullet}$, and the dynamic changes of intermediates of 4-CP.

2. Experimental

2.1. Materials

Na^+-bentonite powder and 4-CP (99%) were purchased from Alfa Aesar (Tianjin, China). Other analytical reagents such as $AlCl_3 \cdot 6H_2O$, $FeCl_3 \cdot 6H_2O$, $CuCl_2 \cdot 2H_2O$, NaOH, H_2O_2 (30 wt.%) and MnO_2 were purchased from Sinopham Chemical Reagent Co., Shanghai, China. Ultrapure water (18.2 MΩ cm, Pall Co., USA) was used in the experiments.

2.2. Preparation of catalysts

The preparation of PILCs was carried out following a conventional pillaring method. Here, chloride solutions with the molar ratio Al/Fe = 5/1, Al/Cu = 5/1, Al/Fe/Cu = 5/0.5/0.5, respectively, were kept at 60 °C and stirred vigorously, followed by dropwise addition of NaOH solution until the molar ratio of titrated amount of OH/(Al + M) reached 2, where M represented Fe or/and Cu. The mixture was continuously stirred and kept at 60 °C for 3 h and then cooled at room temperature.

An aqueous dispersion of bentonite (2 wt.%) which was previously dispersed through continuous stirring the dispersion for 24 h was added dropwise into the pillaring solution mentioned above until the ratio of (Al + M)/clay reached 10 mmol/g, where the mixture was stirred vigorously and kept at 80 °C. After the addition of bentonite dispersion was completed, the mixture was continuously stirred and kept at 80 °C for 3 h and then aged at room temperature for 24 h in the presence of the mother liquor.

The solid was recovered by centrifugation and washed with ultrapure water until chloride-free, then it was dried at 60 °C and finally was calcined at 200, 300, 400, 500, 700 and 900 °C for 2 h, respectively, with the heating rate of 2 °C min^{-1}. The obtained catalyst was designed as Al-M-PILC (T), where T was the value of centigrade temperature.

2.3. Characterization of catalysts

The morphology and elemental composition of the solids were characterized by a field emission scanning electron microscope with an energy-dispersive X-ray spectroscopy (FE-SEM-EDX, Hitachi S-4800). Powder X-ray diffraction (XRD) study was done in a Shimadzu XRD-7000 diffractometer under the following conditions: 40 kV, 30 mA, Cu K_α radiation (λ = 0.15405 nm). Fourier transform infrared (FT-IR) spectra were obtained in 4000–400 cm^{-1} range on a FT/IR 4100 spectrometer (JASCO Benelux BV) using KBr pellet technique. Thermogravimetric analysis (TGA) was performed with a Mettler-Toledo TGA/DSC 1 thermogravimetric analyzer, which operated in a static atmosphere of air, with the heating rate of 10 °C min^{-1} from ambient temperature to 1000 °C. In addition, the specific surface area (SSA) was also measured using an Autosorb-1-MP 1530VP.

2.4. Catalytic oxidation of 4-CP by H_2O_2

The reaction was carried out in a 250-mL three-neck glass flask fitted with a reflux condenser, a magnetic stirrer and a thermostated water bath. For a typical run, 150 mL 4-CP (2.76 mM) and catalyst (0.15 g) in powder form were loaded into the flask. After the reaction mixture was magnetically stirred and heated to the desired temperature (40 °C), H_2O_2 (5.44 mmol) was added at once, which initiated the reaction. During all the oxidation reactions, an aliquot of reactant was withdrawn at selected time intervals, and divided into two groups. One group was mixed with 0.1 g manganese dioxide for the purpose of eliminating residual H_2O_2 (Liou and Chen, 2009; Mei et al., 2004), and filtered by means of 0.22 μm membranes to analyze 4-CP and its intermediates, total organic carbon (TOC), Cl^- and iron and copper; the other was directly filtered to determine residual H_2O_2.

2.5. Analytical methods

4-CP was analyzed in ultra-performance liquid chromatography (UPLC, ACQUITY UPLC H-Class). TOC was measured by Shimadzu TOC-5000 Analyzer. Dissolved metals (Fe or/and Cu) were determined via ICP-MS (ELAN DRC II). Cl^- was measured by ion chromatography (Dionex ICS3000). Solution pH was monitored with Metrohm 888 Titrando. H_2O_2 was analyzed by UV-Vis spectrophotometer (U-3900H) based on the formation of red–orange color peroxovanadium cation after the reaction of H_2O_2 with NH_4VO_3 in acidic medium (Nogueira et al., 2005). According to the method of Robert et al. (2002), $HO^{\bullet}$ was detected by electron spin resonance spectroscopy (ESR, Bruker

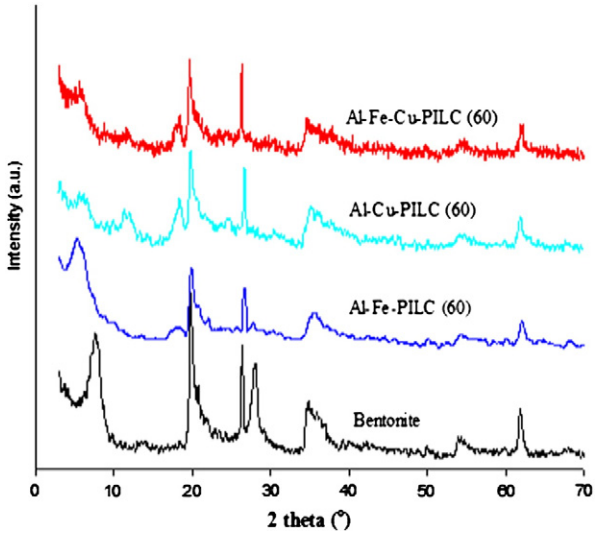

Fig. 1. X-ray diffraction spectra of fresh clay catalysts.

Table 1
Characterization of fresh clay catalysts.

Catalyst	d_{001} (nm)	SSA ($m^2\ g^{-1}$)	Elemental composition (wt.%)								
			O	Si	Al	Na	Mg	Fe	Cu	Cl	Total
Bentonite	1.15	21	57.4	27.4	10.0	1.8	1.5	1.9	–	–	100.0
Al-Fe-PILC (60)	1.67	210	60.9	20.1	12.5	0.1	1.1	4.9	–	0.4	100.0
Al-Cu-PILC (60)	1.42	74	59.2	19.0	15.3	0.2	0.9	2.2	2.0	1.3	100.1
Al-Fe-Cu-PILC (60)	1.57	136	61.8	17.1	13.7	–	1.0	4.4	1.3	0.8	100.1

E500-10/12) coupled to the spin trapping technique using 5,5-dimethyl 1-pyrroline *N*-oxide (DMPO) as spin trap agent.

In order to reveal the oxidation pathway of 4-CP, we detected the course of 4-CP conversion and the appearance of intermediates by UPLC-Q-TOF (Synapt HDMS).

3. Results and discussion

3.1. Characterization of Al-Fe-, Al-Cu-, and Al-Fe-Cu-PILCs

Powder XRD patterns of the fresh catalysts (Fig. 1) were similar to those reported in the literature for Al-Fe-PILC and Al-Cu-PILC (Caudo et al., 2007; Kim and Lee, 2004; Luo et al., 2009; Mojović et al., 2009). The peak at $2\theta = 7.66^{o}$ of raw clay (Na^{+}-bentonite) was attributed to the basal space (001) reflection, which corresponded to a d-value of 1.15 nm. Upon pillaring with Al and Fe or/and Cu, the (001) reflections shifted to lower 2θ values, corresponding to the increase in d_{001} value; while the rest of the structures was not clearly affected, as shown by Kim and Lee (2004). However, a new reflection appeared at around $2\theta = 12.7^{o}$ in the patterns of those samples with copper, maybe attributed to an amorphous hydroxide of copper such as $Cu(OH)_2 \cdot H_2O$ (JCPDS 42-0746) (Lu et al., 2004). Table 1 summarized the results of d_{001} value, SSA and elemental composition. The d_{001} value and SSA, as well as the content of Al and Fe or/and Cu, all increased significantly after pillaring, which indicated iron and copper were efficiently intercalated into the interlayer space of clay. Some study showed that Cu could not be pillared efficiently in the clays (Barrault et al., 1998). However, we here evidenced that Cu could be intercalated in an amount of 2 wt.%, similar to that obtained by Caudo et al. (2007). Additionally, EDX analysis (Table 1) over a number of selected areas exhibited a nearly uniform distribution of Fe or/and Cu throughout the external surface area, which implied that the preparation procedure was efficient for obtaining highly dispersed metal-active species.

According to SEM data (Fig. 2), the raw clay was typical layer structure, with smooth surface. However, the surface of PILCs especially Al-Fe-PILC became very rough and highly porous, with the scrolling delaminated structure in flocculated clays. These results agreed well with the SSA data (Table 1), in which the SSA of PILCs could increase by several times.

The FT-IR spectra of these samples were shown in Fig. 3. The absorption band at 3621 cm^{-1} was due to the stretching vibration of structural OH group (Al-OH) of Na^{+}-bentonite; the bands at 3432 and 1631 cm^{-1} corresponded to the stretching and bending vibrations of H_2O, respectively; the band at 1045 cm^{-1} represented the stretching vibration of Si-O, while the band corresponding to Al-Al-OH bending vibration was observed at 921 cm^{-1}; the band at 790 cm^{-1} implied quartz admixture in the samples; the bands at 528 and 466 cm^{-1} were associated with the bending vibrations of Si-O-Mg and Si-O-Fe, respectively (Eren and Afsin, 2008; Liu et al., 2010; Wang et al., 2009; Yuan et al., 2008). After clay was pillared, the amount of OH groups (H-OH and Al-OH) increased markedly on account of the much stronger absorption at 1631, 3432 and 3621 cm^{-1}. In addition, when Cu was intercalated into clay, a band at 725 cm^{-1} was observed which was probably related to the vibration of Si-O-Cu.

The TGA curves in air of these catalysts (Fig. 4) could be divided into three stages: (1) dehydration of hygroscopic (105 °C) and cation-

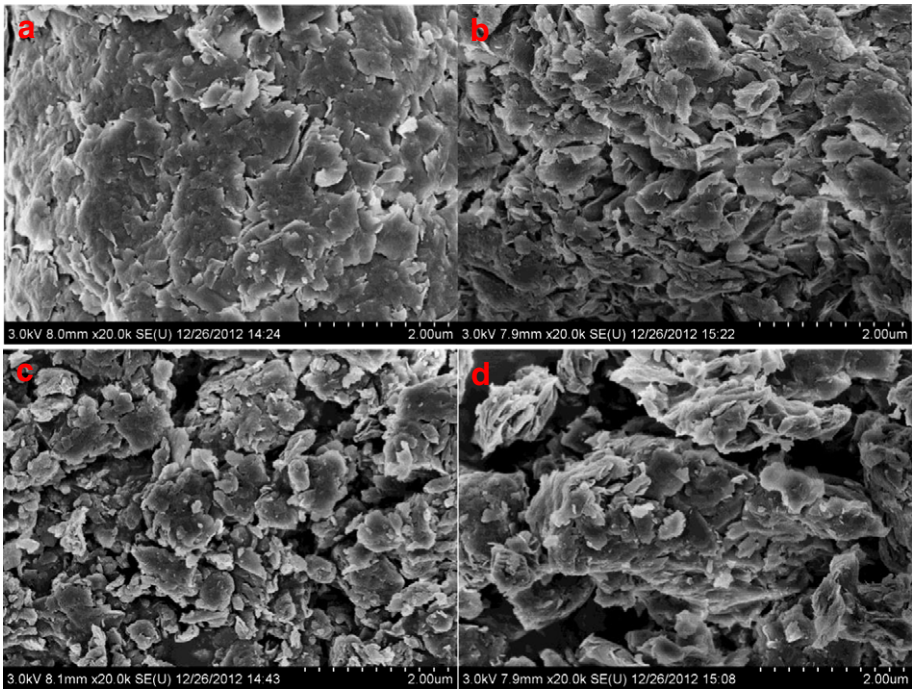

Fig. 2. SEM images of fresh clay catalysts: (a) Bentonite; (b) Al-Fe-PILC (60); (c) Al-Cu-PILC (60) and (d) Al-Fe-Cu-PILC (60).

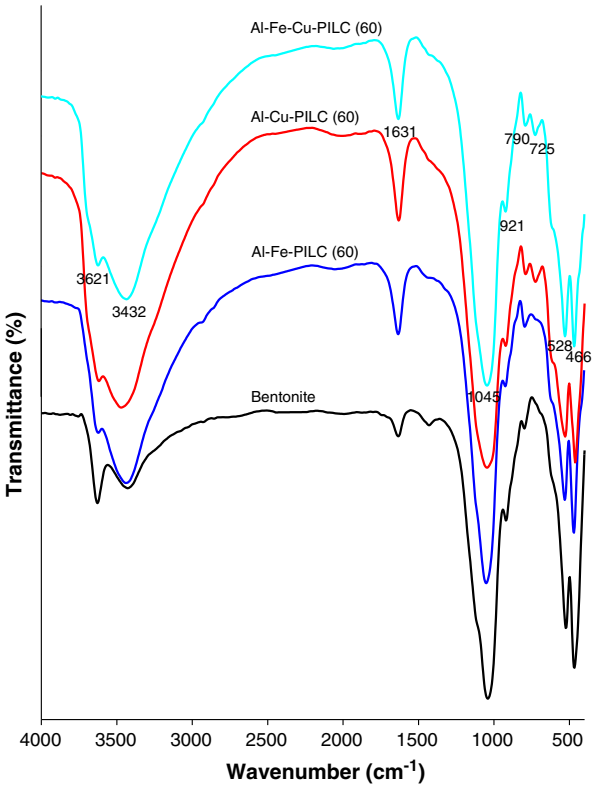

Fig. 3. FT-IR spectra of fresh clay catalysts.

hydrated water (250 °C); (2) dehydroxylation of structural OH groups (660 °C), and (3) the collapse of clay layers (870 °C) (Liu et al., 2014). Apparently, Al-Fe-PILC possessed more hygroscopic water whereas Al-Cu-PILC had more cation-hydrated water, implying that more significant changes occurred at lower temperature (≤200 °C) for the former and higher temperature (200 ~ 500 °C) for the latter. It was interesting to note that there was remarkable mass loss at 380 °C for those samples with copper, being attributed to the chemical transformation of amorphous hydroxide of copper ($Cu(OH)_2 \cdot H_2O$) because the reflection disappeared above 300 °C (Fig. 5). It could be also observed from Fig. 5 that the (060) reflection ($2\theta = 62^o$) of Al-Fe-PILC remained up to 700 °C whereas it in Al-Cu-PILC disappeared above 500 °C, indicating that the dehydroxylation began at temperature above 500 °C for Al-Cu-PILC and 700 °C for Al-Fe-PILC, respectively (Liu et al., 2014).

Although the reason why the (001) reflection was more intense with increase in calcination temperature and remained up to higher temperature (700 °C) was unclear, Al-Cu-PILCs experienced indeed more structural changes (modification) under heating, as proved by TGA and XRD (Figs. 4 and 5), meaning higher structural sensitivity to thermal changes. Additionally, that their SSA increased markedly when the calcination temperature was increased from 300 to 500 °C (Table 2) also provided a strong support.

3.2. Kinetics of the oxidation of 4-CP by H_2O_2 over PILCs

When they were used in the wet oxidation of 4-CP, Al-Fe-, Al-Cu- and Al-Fe-Cu-PILCs exhibited high catalytic activity, as shown in Fig. 6. It was seen that 4-CP could be completely oxidized within 2 h. While our previous preliminary tests demonstrated that 4-CP could not be oxidized by H_2O_2 in the absence of clay catalysts; and the removal of 4-CP caused by adsorption on the clays was also negligible (Zhou et al., 2011a).

The Fenton-like reaction here showed an induction period followed by a rapid oxidation, yielding an S-shape profile of concentration versus time (Fig. 6). In fact, during the catalytic reaction the induction period was often observed (Belaroui and Bengueddach, 2012; Carriazo et al., 2003; Catrinescu et al., 2012; Kurian and Sugunan, 2006; Luo et al., 2009; Park and Baker, 2002; Timofeeva et al., 2005; Velegraki et al., 2011), but its cause was unclear due to little discussion on the intricate reaction involving catalyst, H_2O_2 and pollutants (Luo et al., 2009; Velegraki et al., 2011). Some study attributed it to the adsorption of phenol and corresponding to the formation of phenoxy radicals on catalytic surface (Carriazo et al., 2003; Kurian and Sugunan, 2006); some considered it as the result of the dissolution of a portion of ferric ions (Belaroui and Bengueddach, 2012; Catrinescu et al., 2012); while Luo et al. (2009) put it down to the protonation of surface iron species since a lower pH shortened the induction period. In short, the detailed investigation to the induction period would be helpful to elucidating the mechanism of heterogeneous catalytic oxidation.

A kinetic model which was based on the Fermi's function was used to describe the oxidation process of 4-CP:

$$\frac{C_t}{C_0} = \frac{1}{1 + \exp[k(t - t_*)]} \quad (1)$$

where k represented the equivalent apparent first-order rate constant (min^{-1}), and t_* was the transition time (min), related with the concentration curve's inflection point (Herney-Ramireza et al., 2011; Silva et al., 2012).

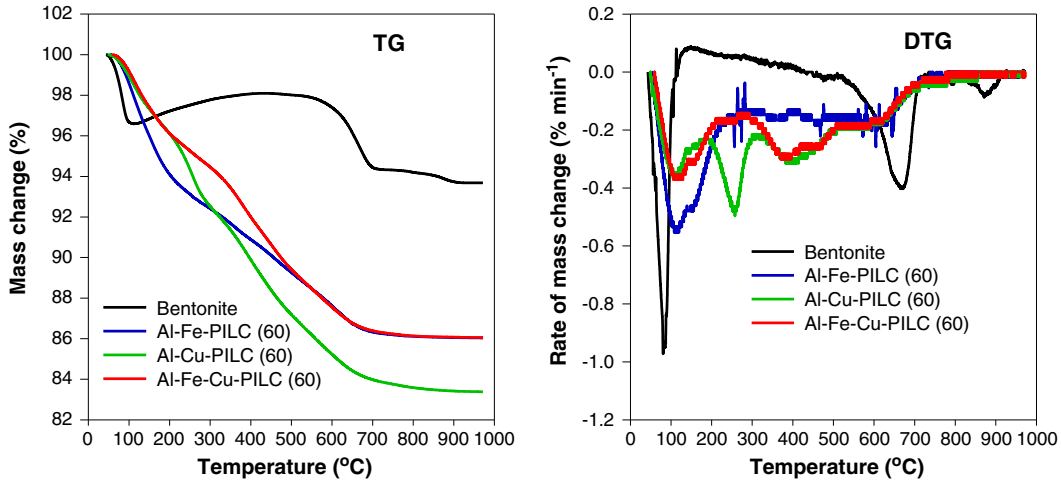

Fig. 4. TG and DGT curves for fresh clay catalysts.

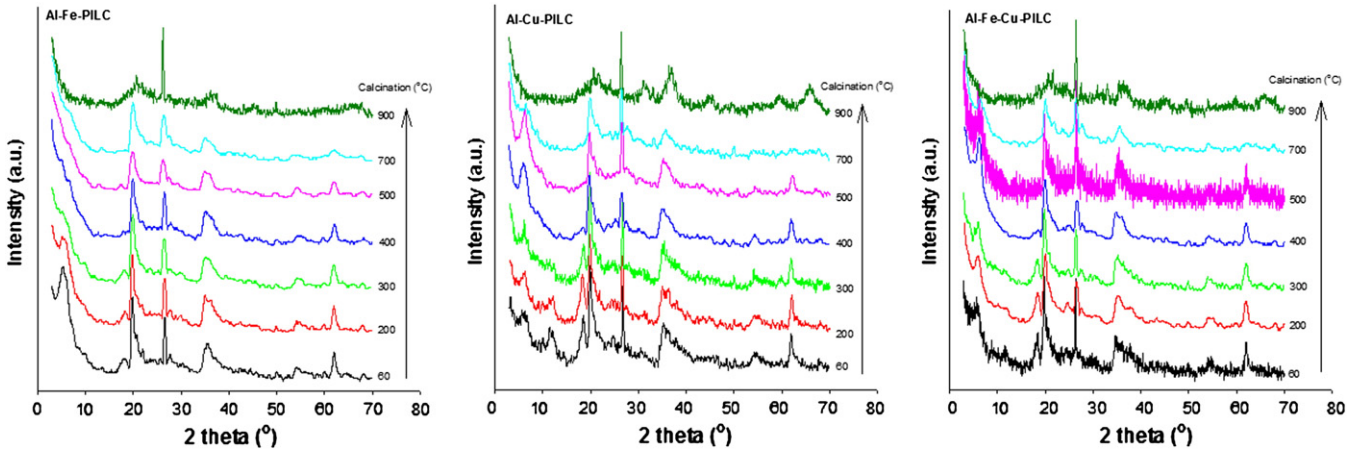

Fig. 5. X-ray diffraction patterns of Al-Fe-, Al-Cu- and Al-Fe-Cu-PILCs with different calcination temperatures.

Further, the induction time (t_I) which could be determined by setting the third differential of the model equal to zero (Luo et al., 2009) was calculated as follows:

$$t_I = t_* + \frac{\ln\left(2-\sqrt{3}\right)}{k} \quad (2)$$

The oxidation processes of 4-CP (Fig. 6) were modeled well, with $R^2 = 0.9938 \sim 0.9993$ and $p < 0.0001$. The obtained k, t_* and t_I for Al-Fe-, Al-Cu- and Al-Fe-Cu-PILCs were 0.139, 0.106, 0.171 min^{-1}; 63, 39, 33 min; 54, 27, 26 min, respectively. It meant that compared to Al-Cu-PILC, Al-Fe-PILC possessed higher catalytic capacity but needed longer time for its activation (longer induction period). In addition, it was also concluded that Fe-Cu bimetal clay catalyst would be optimal because of combining the advantages of both Al-Fe-PILC (higher k) and Al-Cu-PILC (shorter t_I).

Some study evidenced that reaction temperature was the most decisive factor affecting the induction period (Luo et al., 2009; Velegraki et al., 2011). Thus, we investigated the effect of reaction temperature on k and t_I, as shown in Fig. 7. It was found that there was good linear relation between ln$k$ (and lnt_I) and 1/T, with $R^2 = 0.9954$ and 0.9796, respectively, and there was very similar to the observations of Luo et al. (2009), in which the equation with the best R^2 of 0.9785 was adopted: $\ln t_I = 8929/T - 26.494$. Based on the linear relation in Fig. 7, further calculation was done to obtain the activation energy (E_a) of 54.87 kJ mol^{-1} for the catalytic oxidation of 4-CP by H_2O_2 over Al-Fe-Cu-PILC (300). The value was slightly higher than that over Cu (II)-kaolinite (43.54 kJ mol^{-1}) and Cu (II)-montmorillonite (40.39 kJ mol^{-1}) (Khanikar and Bhattacharyya, 2013), probably due to the milder conditions in our reaction system.

Table 2 and Fig. 8 were the results of effects of calcination temperature on the structure and activity of PILCs. Obviously, there was significantly different structural and active sensitivity for Al-Fe-PILC and Al-Cu-PILC, strongly depending on the calcination temperature. Although it exhibited higher activity (higher k and TOC conversion), there was usually longer time needed for activation of Al-Fe-PILC, and what was more important was that the activity decreased sharply with calcination temperature so that almost 100% of its activity was lost above 700 °C. On the contrary, Al-Cu-PILC not only retained higher activity after the collapse of clay layers (900 °C) but also showed a slight increase in its activity at 200–500 °C pretreatment (Table 2 and Fig. 8). Generally, the significant active difference affected by calcination temperature among PILCs was ascribed to their structural changes but not

Table 2
Catalytic wet peroxide oxidation of 4-CP over PILCs at 40 °C for 2 h ([4-CP] = 2.76 mM; [H_2O_2] = 36.27 mM; [catalyst] = 1 g L^{-1}).

Catalyst	d_{001} (nm)	SSA (m^2 g^{-1})	Reaction kinetics of 4-CP				TOC conversion (%)	Active metallic leaching (mg L^{-1})		
			Conversion (%)	k (min^{-1})	t_* (min)	t_I (min)		Fe	Cu	Total
Al-Fe-PILC (60)	1.67	210	100	0.139	63	54	65.6	1.35	0	1.35
Al-Fe-PILC (200)	1.67	198	100	0.235	37	31	72.6	3.23	0	3.23
Al-Fe-PILC (300)	1.71	191	100	0.214	36	29	71.5	1.46	0	1.46
Al-Fe-PILC (400)	1.46	195	100	0.153	33	24	67.7	2.41	0	2.41
Al-Fe-PILC (500)	–	193	100	0.191	42	35	61.9	2.52	0	2.52
Al-Fe-PILC (700)	–	153	5.7	Not applicable			5.8	0	0	0
Al-Fe-PILC (900)	–	17	4.1	Not applicable			1.2	0	0	0
Al-Cu-PILC (60)	1.42	74	100	0.106	39	27	54.7	0.39	4.04	4.43
Al-Cu-PILC (200)	1.46	73	100	0.117	38	27	56.3	0.38	3.17	3.55
Al-Cu-PILC (300)	1.46	85	100	0.104	38	25	55.2	0	2.03	2.03
Al-Cu-PILC (400)	1.47	88	100	0.078	39	23	56.9	0	1.90	1.90
Al-Cu-PILC (500)	1.42	91	100	0.118	31	20	58.3	0.22	2.28	2.50
Al-Cu-PILC (700)	1.33	65	100	0.107	39	27	45.5	0.49	2.16	2.65
Al-Cu-PILC (900)	–	19	85.6	0.040	77	45	24.2	0	0.13	0.13
Al-Fe-Cu-PILC (60)	1.57	136	100	0.171	33	26	62.7	2.98	1.20	4.18
Al-Fe-Cu-PILC (200)	1.51	136	100	0.189	36	29	64.9	2.41	0.73	3.14
Al-Fe-Cu-PILC (300)	1.46	133	100	0.304	24	19	68.0	4.93	0.88	5.81
Al-Fe-Cu-PILC (400)	1.45	142	100	0.246	26	21	64.9	2.27	1.36	3.63
Al-Fe-Cu-PILC (500)	1.45	142	100	0.246	21	16	63.6	1.97	0.82	2.79
Al-Fe-Cu-PILC (700)	1.42	115	99.9	0.174	38	30	54.0	2.37	1.44	3.81
Al-Fe-Cu-PILC (900)	–	16	95.2	0.058	56	34	34.4	0	0.13	0.13

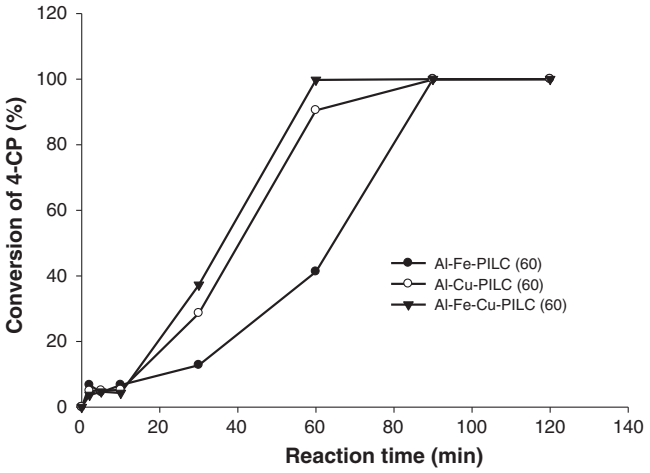

Fig. 6. Kinetics of catalytic wet peroxide oxidation of 4-CP over PILCs (Reaction conditions: [4-CP] = 2.76 mM; [H_2O_2] = 36.27 mM; [catalyst] = 1 g L^{-1}; temperature of 40 °C).

to the leaching of active metal ions during CWPO of 4-CP (metal dissolution was low and was not defined as the cause initiating the oxidation reaction, which would be stated in the following section). Al-Cu-PILCs experienced more structural changes (modifications) under heating, as mentioned above section, assuredly resulting in different response to calcination temperature from Al-Fe-PILCs. Thus, the structural evolution under thermal treatments and structure–activity relationships of copper-based clay catalysts should be paid more attention in the future for high performance catalyst materials.

In view of the apparent rate constant (k) and the conversion rate of TOC (Table 2), we suggested that the optimized calcination temperature was 200 °C for Al-Fe-PILC, 300 °C for Al-Fe-Cu-PILC and 500 °C for Al-Cu-PILC, respectively. Almost the same trend was observed with respect to SSA of PILCs (Table 2), which revealed again a high degree of consistency between active sensitivity and structural sensitivity of clay catalysts. This result was consistent with earlier findings that SSA of Al-Cu-PILC increased up to 500 °C, whereas that of fresh Al-Fe-PILC continuously decreased in function of pretreatment temperature (Marinkovic-Neducin et al., 2004). Vicente et al. (2001) also confirmed that the intercalated clays showed important modifications of their structural characteristics on heating at 300 or 500 °C. However, this study indicated that there were also some inconsistencies and nonsignificant relationships among the structure and activity of PILCs and the leaching of metal ions (Table 2), which meant the complicacies of heterogeneous catalytic reaction. So, further study should be done on the relationships between fine microstructure and catalytic activity of PILCs in the future.

3.3. Mechanism of catalytic wet peroxide oxidation of 4-CP

Fig. S1 showed ESR spectra during the reaction of DMPO in water and 4-CP solution, respectively, over Al-Fe-Cu-PILC (300)/H_2O_2 system. The four-line signal pattern of DMPO-HO• could be observed, and in the presence of 4-CP, its signal decreased significantly, indicating that Al-Fe-Cu-PILC catalyst was capable of generating HO•, and thus initiating the oxidation of 4-CP (Kim and Metcalfe, 2007). Although Tatibouët et al. (2005) considered that the nature of the active oxygen species responsible of this Fenton-like reaction remained questionable because various oxygen species such as HO•, HO_2• and O_2^-• could lead to the final formation of DMPO-HO•, the reaction mechanism of free-radical oxidation was never in doubt. The correlations among HO• concentration related to the maximum of DMPO-HO• signal amplitude (Kochany and Bolton, 1992), conversion of 4-CP and TOC, and reaction time were illustrated in Fig. 9. It was found that the conversion of 4-CP and TOC and the generation of HO• increased synchronously within 50 min, suggesting again the oxidation from HO• produced by the surface-catalyzed decomposition of H_2O_2.

Fig. 10 was the interdependence among H_2O_2 decomposition, 4-CP oxidation, metallic dissolution, Cl^- release and pH change. It indicated incontestably that the dissolution of metal ions (Fe or/and Cu) was not the reason for initiating the Fenton-like reaction, as suggested by Belaroui and Bengueddach (2012), but the result of a sharp decrease of solution pH caused by surface-catalyzed reaction, because when the dissolution of metals took place (30 min), 4-CP was almost oxidized completely (87.5%). Thus, the induction period observed should be attributed to the activation of the catalyst surface, as described in following reactions (Huang and Huang, 2008; Kwan and Voelker, 2003):

$$\equiv Fe^{III} + H_2O_2 \rightarrow \equiv Fe^{III}H_2O_2 \quad (3)$$

$$\equiv Fe^{III}H_2O_2 \rightarrow \equiv Fe^{II} + HO_2\bullet + H^+ \quad (4)$$

$$\equiv Fe^{II} + H_2O_2 \rightarrow \equiv Fe^{III} + HO\bullet + OH^- \quad (5)$$

Timofeeva et al. (2005) confirmed by ESR and DR-UV-Vis spectra the formation of peroxide-Fe^{3+} complex upon the interaction of H_2O_2 and

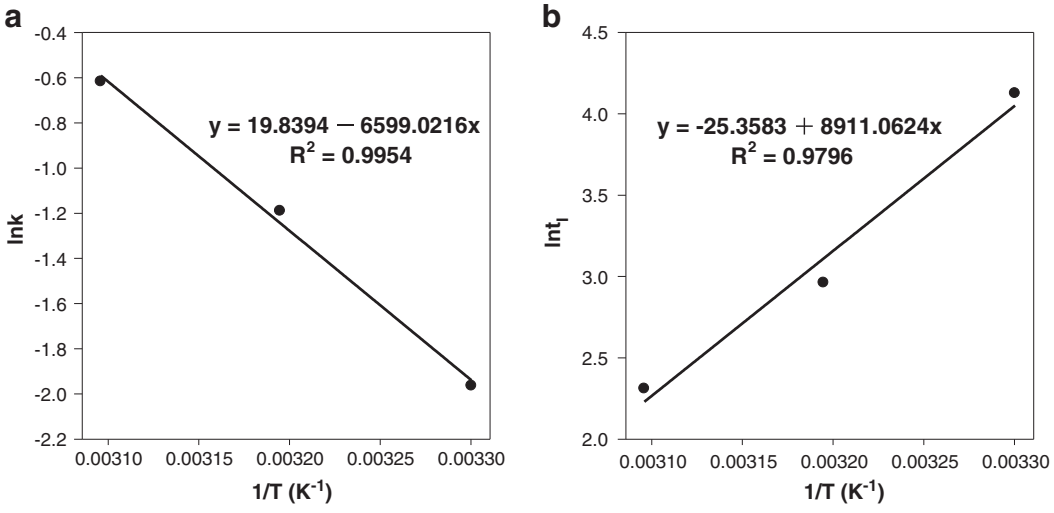

Fig. 7. (a) Arrhenius plot for the apparent rate constants of the oxidation of 4-CP over Al-Fe-Cu-PILC (300) and (b) effect of temperature on the induction time (t_I). The lines represented the linear regression fittings (Reaction conditions: [4-CP] = 2.76 mM; [H_2O_2] = 36.27 mM; [catalyst] = 1 g L^{-1}).

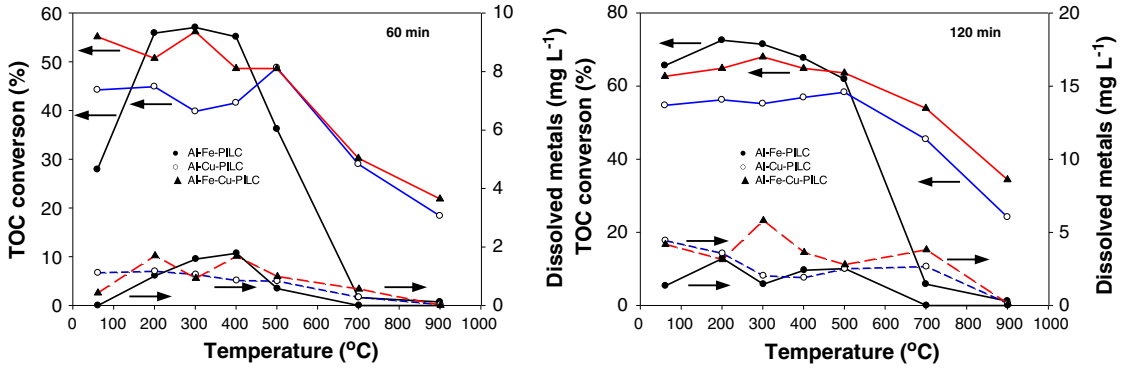

Fig. 8. Effect of calcination temperature on TOC conversion and metallic dissolution (Reaction conditions: [4-CP] = 2.76 mM; [H_2O_2] = 36.27 mM; [catalyst] = 1 g L^{-1}; temperature of 40 °C).

Al-Fe-PILC. It was assumed that reaction (4) was the rate-limiting step (Kwan and Voelker, 2003), therefore, at the initial stage of the catalytic reaction (induction period), pH rapidly and incessantly decreased along the adsorption and sequent decomposition of H_2O_2, as shown in Fig. 10.

Fig. 10 also showed that the concentration of H_2O_2 continually decreased with reaction time, following pseudo-first order kinetics (k = 0.0085 min^{-1}, R^2 = 0.9916) (Hiroki and LaVerne, 2005; Huang and Huang, 2008). But the consumption rate of H_2O_2 did not equal the generation rate of HO• (Fig. 9), because H_2O_2 could be decomposed to water and oxygen via a non-radical-producing pathway (Huang and Huang, 2008; Kwan and Voelker, 2003), or not HO• but other radicals such as HO_2• formed, as described in the reaction (4). Tatibouët et al. (2005) found that the pH of the reaction played an important role in the generation of HO•, where a maximum of HO• production was observed for a pH value around 3.7. So, during the induction period little or no HO• generated in view of the higher pH in reaction system, correspondingly causing little or no oxidation of 4-CP; after the induction period (19 min), a large number of HO• generated due to the lower pH (≤4), resulting in the rapid and complete oxidation of 4-CP (Figs. 9 and 10). After a longer time of reaction such as 60 min, on the one hand the amount of residual H_2O_2 was small, on the other hand the value of solution pH became less than 2.3, the generation rate of HO• would be slow again (Fig. 9). To sum up, HO• generated via the catalytic decomposition of H_2O_2 over heterogeneous catalysts determined the process and mechanism of oxidation of organic pollutants; the occurrence of induction period was to adjust the acidity of reaction system to the optimum where a large number of HO• could generate rapidly, promoting the degradation of organics.

Of course, we did not rule out this possibility where dissolved metal ions (Fe or Cu) took part in the deep oxidation of 4-CP in the second half of whole catalytic reaction, due to a large number of Cl^- release and more TOC conversion, as combined heterogeneous-homogeneous mechanism for the whole reaction system, proposed by some researchers (Catrinescu et al., 2012; Huang and Huang, 2008). However, the results of our study at least proved that at initial reaction (induction period) it was only the heterogeneous surface activation and catalysis which regulated the oxidation of 4-CP.

Further investigation on the morphology and elemental composition of Al-Fe-Cu-PILC (300) before and after reaction (Fig. 11 and Table 3) provided also evidence in favor of the surface-catalyzed reaction. After 6 runs the catalyst surface became smooth probably owing to the deposits of a certain amount of carbon (8%); additionally, the content of active metals especially Fe decreased markedly. These factors would lead to the decrease of catalytic activity. Accordingly, it could be concluded that surface-catalyzed decomposition of H_2O_2 provided HO• that attacked 4-CP in solution or adsorbed on catalyst surface, resulting in a certain amount of intermediates such as oxalic acid remaining or adsorbing on the solid surface by its complexation with Fe (III) (Huang and Huang, 2008).

During deep oxidation stage (after completing 4-CP degradation reaction), more than 60% of chlorine atoms was dechlorinated; in particular, during rapid oxidation of 4-CP, only 10% of chlorine atoms was dechlorinated (Fig. 10). It meant that main intermediates of 4-CP degradation were chlorinated products such as 4-chlorocatechol

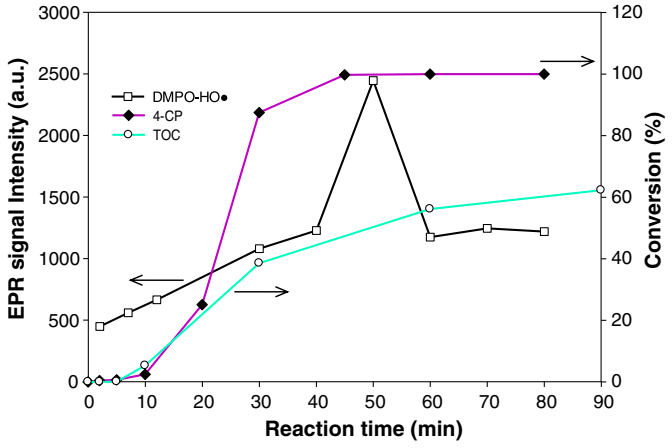

Fig. 9. Time-dependent correlation between formation of HO• and conversion of 4-CP and TOC by H_2O_2 over Al-Fe-Cu-PILC (300) (Reaction conditions: [4-CP] = 2.76 mM; [H_2O_2] = 36.27 mM; [catalyst] = 1 g L^{-1}).

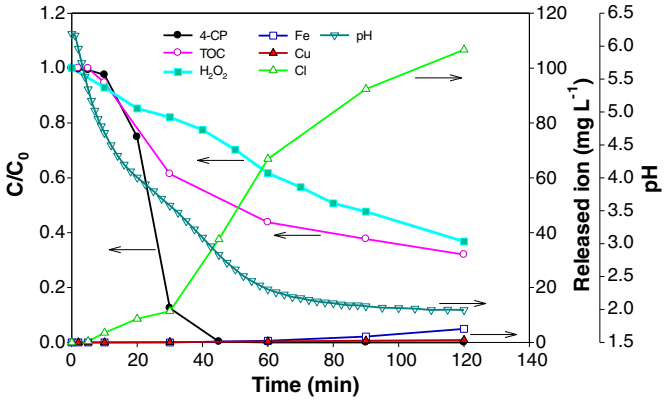

Fig. 10. Profiles of H_2O_2 decomposition, metallic dissolution, Cl^- release and pH changes during catalytic reaction of 4-CP over Al-Fe-Cu-PILC (300) (Reaction conditions: [4-CP] = 2.76 mM; [H_2O_2] = 36.27 mM; [catalyst] = 1 g L^{-1}; temperature of 40 °C).

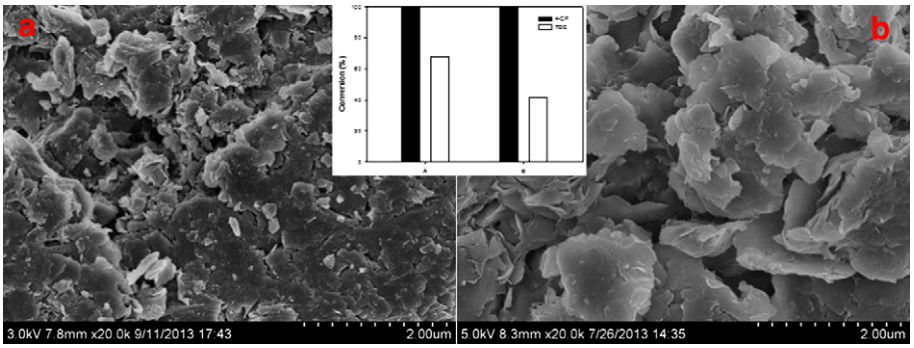

Fig. 11. SEM micrographs for Al-Fe-Cu-PILC (300): (a) before reaction; (b) after six runs. The inserted chart is the conversion of 4-CP and TOC in first run (A) and sixth run (B), respectively (Reaction conditions: [4-CP] = 2.76 mM; [H_2O_2] = 36.27 mM; [catalyst] = 1 g L^{-1}; temperature of 40 °C, and time of 2 h).

(4-CC). But during induction period small amount of 4-CP was completely dechorinated (Fig. 10), along the formation of non-chlorinated products such as hydroquinone. Some study supposed two major pathways: (A) the formation of 4-CC as the result of HO• attack at *ortho* position to the hydroxyl group; (B) the formation of hydroquinone due to HO• attack at *para* position on the ring (Catrinescu et al., 2011; Chaliha et al., 2008; Li et al., 1999). Usually HO• attack did take place more readily at *ortho* position (Catrinescu et al., 2011), thus, 4-CC was dominant pathway of degradation. Chaliha et al. (2008) considered that on further oxidation, hydroquinone was converted to *p*-benzoquinone, which was easily oxidized to maleic acid, and finally low molecular mass organic acids such as oxalic acid, formic acid and acetic acid formed. This was very similar to the oxidation pathway of phenol (Quintanilla et al., 2010; Zhou et al., 2011b; Zrnčević and Gomzi, 2005), but in fact the oxidation of 4-CP was much more complex than that of phenol. On the one hand the formation of hydroquinone was not dominant pathway; on the other hand the hydroxylation and chlorination of hydroquinone was probably to take place, leading to the formation of more complex compounds (Catrinescu et al., 2011; Li et al., 1999). Li et al. (1999) investigated in detail the photocatalytic degradation pathway of 4-CP, and showed that 1,2,4-benzentriol and 3-hydroxymuconic acid, 5-chloro-1,2,4-benzentriol and 4-chloro-3-hydroxymuconic acid were main intermediates of pathway (B) and (A), respectively. Fig. S2 exhibited the changes of intermediates of 4-CP oxidation by H_2O_2 over PILCs with reaction time. By the analysis of UPLC-Q-TOF mass spectrometry we detected besides 4-CP (m/z = 126.99, 128.99) several major and minor intermediates listed in the literature (Catrinescu et al., 2011; Chaliha et al., 2008; Li et al., 1999), supporting the oxidation pathway of 4-CP, as proposed by Li et al. (1999).

However, some major mass spectral characteristic ions extracted from Fig. S2 such as m/z = 186.86, 202.94, 213.88, 240.90, 252.98 and 254.98 were unable to be identified. Catrinescu et al. (2011) considered that high molecular mass compounds (dimers, oligomers) probably formed by oxidative coupling reaction during CWPO of 4-CP, for example dichlorodihydroxybiphenyl, dihydroxytrichlorobiphenyl, etc. The molecular mass (MM = 256.10) of dichlorodihydroxybiphenyl was very consistent with the protonated molecular ions at m/z = 252.98 and 254.98. Maybe, in our reaction system the further more complex hydroxylation and chlorination of 4-CP or its major intermediates occurred, along the degradation processes (dechlorination and cleavage of the aromatic ring).

Fig. S2 showed the same trend of 4-CP oxidation over Al-Fe-PILC and Al-Cu-PILC, where 4-CP was gradually oxidized into two main products besides CO_2, H_2O and Cl^-: I (m/z = 159.84, 161.84) and II (m/z = 202.94). But, there was also marked difference in 4-CP oxidation over the two types of PLICs, where compound II accounted for a considerable proportion for Al-Fe-PILC, even became main component for Al-Fe-Cu-PILC, whereas compound I was almost the only component for Al-Cu-PILC (Fig. S2). Based on the data of pH decrease and Cl^- release (Fig. 10), it was assumed that compounds I and II should be acid-related substances. Further, compound I might be identified as 2,4-dioxopentanedioic acid (MM = 160.08); compound II was speculated to be some ferric-oxalate complex since it was closely related to Fe (Huang and Huang, 2008) and more oxalic acid generated in Al-Fe-PILC (Caudo et al., 2007).

Table 3
The chemical composition (wt.%) of Al-Fe-Cu-PILC (300) before and after reaction by EDX analysis.

	C	O	Si	Al	Mg	Fe	Cu	Cl	Total
Before reaction	–	56.4	21.8	13.8	1.1	4.6	1.5	0.8	100.0
After 6 runs	8.0	52.1	23.3	12.1	1.0	2.2	1.2	0.1	100.0

4. Conclusions

Al-Fe-, Al-Cu-, and Al-Fe-Cu-PILCs was synthesized and characterized by XRD, SEM-EDX, SSA, FT-IR and TGA measurements. The kinetics and mechanism of 4-CP oxidation were investigated, and the structural and active differences between Al-Fe-PILC and Al-Cu-PILC were also studied. The results showed that the oxidation of 4-CP with an apparent induction period could be modeled well using a Fermi' kinetic equation (R^2 = 0.9938 ~ 0.9993), and the activation energy calculated was 54.87 kJ mol^{-1}. Compared to Al-Cu-PILC, Al-Fe-PILC exhibited higher catalytic activity (higher *k* and TOC conversion) but needed longer time for activation (higher t_l). In addition, the optimal calcination temperature was different for the two types of PILCs, with 200 °C for Al-Fe-PILC and 500 °C for Al-Cu-PILC. Surface-catalyzed decomposition of H_2O_2 into $HO^\bullet$ was the oxidation cause whereas the dissolution of active metals (Fe or/and Cu) was its result, so the induction period was attributed to heterogeneous surface activation (catalysis or modification) where the pH of reaction system was sharply reduced to 3 ~ 4 for generating more $HO^\bullet$. The catalytic oxidation of 4-CP was very complex, in which not only dechlorination but also hydroxylation and chlorination occurred. Generally, it proceeded via 4-chlorocatechol (major) and hydroquinone (minor) pathways, where 5-chloro-1,2,4-benzentriol was main intermediate. Upon further oxidation, 4-CP was transformed into besides CO_2, H_2O and Cl^- two main compounds (I and II) as acid-related substances. Additionally, compound II assumed as ferric-oxalate complex accounted for a considerable proportion in Al-Fe-PILC/H_2O_2-4-CP system, whereas compound I identified as 2,4-dioxopentanedioic acid was almost only component in Al-Cu-PILC/H_2O_2-4-CP system.

In short, this study provided strong support for the surface-catalyzed reaction among PILCs, H_2O_2 and 4-CP, and revealed the differences in structural and catalytic sensitivity between Al-Fe-PILC and Al-Cu-PILC. It would be helpful to the catalytic abatement of real CP-bearing

wastewater using PILCs under milder conditions. Further studies should be conducted towards the understanding of the fine surface microstructure of PILCs and of the structure-activity relationships in various reaction conditions.

Acknowledgements

This work was financially supported by National Natural Science Foundation of China (41271254) and Key Laboratory of Soil Environmental and Pollution Remediation, Institute of Soil Science, Chinese Academy of Sciences. The authors thank Dr. Ying Liu for UPLC analysis, Dr. Wenhai Wang for SEM-EDX analysis, Dr. Yang Tan for TGA and TOC analysis, and Dr. Chengli Qu for the measurement of elemental concentration.

Appendix A. Supplementary data

Supplementary data to this article can be found online at http://dx.doi.org/10.1016/j.clay.2014.04.024.

References

Barrault, J., Bouchoule, C., Echachoui, K., Frini-Srasra, N., Trabelsi, M., Bergaya, F., 1998. Catalytic wet peroxide oxidation (CWPO) of mixed (Al-Cu)-pillared clays. Appl. Catal. B Environ. 15, 269–274.

Belaroui, L.S., Bengueddach, A., 2012. Study of the catalytic activity of Al-Fe pillared clays in the Baeyer–Villiger oxidation. Clay Miner. 47, 275–284.

Carriazo, J.G., Guélou, E., Barrault, J., Tatibouët, J.M., Moreno, S., 2003. Catalytic wet peroxide oxidation of phenol over Al-Cu or Al-Fe modified clays. Appl. Clay Sci. 22, 303–308.

Catrinescu, C., Arsene, D., Teodosiu, C., 2011. Catalytic wet hydrogen peroxide oxidation of para-chlorophenol over Al/Fe pillared clays (AlFePILCs) prepared from different host clays. Appl. Catal. B Environ. 101, 451–460.

Catrinescu, C., Arsene, D., Apopei, P., Teodosiu, C., 2012. Degradation of 4-chlorophenol from wastewater through heterogeneous Fenton and photo-Fenton process, catalyzed by Al-Fe PILC. Appl. Clay Sci. 58, 96–101.

Caudo, S., Centi, G., Genovese, C., Perathoner, S., 2007. Copper- and iron-pillared clay catalysts for the WHPCO of model and real wastewater streams from olive oil milling production. Appl. Catal. B Environ. 70, 437–446.

Caudo, S., Genovese, C., Perathoner, S., Centi, G., 2008. Copper-pillared clays (Cu-PILC) for agro-food wastewater purification with H_2O_2. Microporous Mesoporous Mater. 107, 46–57.

Chaliha, S., Bhattacharyya, K.G., Paul, P., 2008. Catalytic destruction of 4-chlorophenol in water. Clean 36, 488–497.

Eren, E., Afsin, B., 2008. An investigation of Cu(II) adsorption by raw and acid-activated bentonite: A combined potentiometric, thermodynamic, XRD, IR, DTA study. J. Hazard. Mater. 151, 682–691.

Galeano, L.A., Gil, A., Vicente, M.A., 2010. Effect of the atomic active metal ratio in Al/Fe-, Al/Cu- and Al/(Fe-Cu)-intercalating solutions on the physicochemical properties and catalytic activity of pillared clays in the CWPO of methyl orange. Appl. Catal. B Environ. 100, 271–281.

Garrido-Ramírez, E.G., Theng, B.K.G., Mora, M.L., 2010. Clays and oxide minerals as catalysts and nanocatalysts in Fenton-like reactions-A review. Appl. Clay Sci. 47, 182–192.

Gil, A., Korili, S.A., Trujillano, R., Vicente, M.A., 2010. Pillared clays and related catalysts. Springer, New York.

Guélou, E., Barrault, J., Fournier, J., Tatibouët, J.M., 2003. Active iron species in the catalytic wet peroxide oxidation of phenol over pillared clays containing iron. Appl. Catal. B Environ. 44, 1–8.

Herney-Ramireza, J., Silva, A.M.T., Vicente, M.A., Costa, C.A., Madeira, L.M., 2011. Degradation of acid orange 7 using a saponite-based catalyst in wet hydrogen peroxide oxidation: Kinetic study with the Fermi's equation. Appl. Catal. B Environ. 101, 197–205.

Hiroki, A., LaVerne, J.A., 2005. Decomposition of hydrogen peroxide at water-ceramic oxide interfaces. J. Phys. Chem. B 109, 3364–3370.

Huang, C.P., Huang, Y.H., 2008. Comparison of catalytic decomposition of hydrogen peroxide and catalytic degradation of phenol by immobilized iron oxides. Appl. Catal. A Gen. 346, 140–148.

Khanikar, N., Bhattacharyya, K.G., 2013. Cu(II)-kaolinite and Cu(II)-montmorillonite as catalysts for wet oxidative degradation of 2-chlorophenol, 4-chlorophenol and 2,4-dichlorophenol. Chem. Eng. J. 233, 88–97.

Khankhasaeva, S.T., Badmaeva, S.V., Dashinamzhilova, E.T., 2008. Preparation, characterization and catalytic application of Fe- and Fe/Al-pillared clays in the catalytic wet peroxide oxidation of 4-chlorophenol. Stud. Surf. Sci. Catal. 174, 1311–1314.

Kim, S.C., Lee, D.K., 2004. Preparation of Al-Cu pillared clay catalysts for the catalytic wet oxidation of reactive dyes. Catal. Today 97, 153–158.

Kim, J.K., Metcalfe, I.S., 2007. Investigation of the generation of hydroxyl radicals and their oxidative role in the presence of heterogeneous copper catalysts. Chemosphere 69, 689–696.

Kochany, J., Bolton, J.R., 1992. Mechanism of photodegradation of aqueous organic pollutants. 2. Measurement of the primary rate constants for reaction of hydroxyl radicals with benzene and some halobenzenes using an EPR spin-trapping method following the photolysis of hydrogen peroxide. Environ. Sci. Technol. 26, 262–265.

Kurian, M., Sugunan, S., 2006. Wet peroxide oxidation of phenol over mixed pillared montmorillonites. Chem. Eng. J. 115, 139–146.

Kwan, W.P., Voelker, B.M., 2003. Rates of hydroxyl radical generation and organic compound oxidation in mineral-catalyzed Fenton-like systems. Environ. Sci. Technol. 37, 1150–1158.

Li, X.J., Cubbage, J.W., Jenks, W.S., 1999. Photocatalytic degradation of 4-chlorophenol. 2. The 4-chlorocatechol pathway. J. Org. Chem. 64, 8525–8536.

Liotta, L.F., Gruttadauria, M., Di Carlo, G., Perrini, G., Librando, V., 2009. Heterogeneous catalytic degradation of phenolic substrates: Catalysts activity. J. Hazard. Mater. 162, 588–606.

Liou, R.M., Chen, S.H., 2009. CuO impregnated activated carbon for catalytic wet peroxide oxidation of phenol. J. Hazard. Mater. 172, 498–506.

Liu, X.W., Liu, Z., Zhong, G., Mao, X.X., 2010. Thermal action of Zr/Al-pillared montmorillonite. J. Cent. South Univ. (Sci. Technol.) 41, 2060–2064 (In Chinese with English abstract).

Liu, H.Y., Shen, T., Li, T.S., Yuan, P., Shi, G., Bao, X.J., 2014. Green synthesis of zeolites from a natural aluminosilicate mineral rectorite: Effects of thermal treatment temperature. Appl. Clay Sci. 90, 53–60.

Lu, C.H., Qi, L.M., Yang, J.H., Zhang, D.Y., Wu, N.Z., Ma, J.M., 2004. Simple template-free solution route for the controlled synthesis of $Cu(OH)_2$ and CuO nanostructures. J. Phys. Chem. B 108, 17825–17831.

Luo, M.L., Bowden, D., Brimblecombe, P., 2009. Catalytic property of Fe-Al pillared clay for Fenton oxidation of phenol by H_2O_2. Appl. Catal. B Environ. 85, 201–206.

Marinkovic-Neducin, R.P., Kiss, E.E., Cukic, T.Z., Obadovic, D.Z., 2004. Thermal behavior of Al-, AlFe- and AlCu-pillared interlayered clays. J. Therm. Anal. Calorim. 78, 307–321.

Mei, J.G., Yu, S.M., Cheng, J., 2004. Heterogeneous catalytic wet peroxide oxidation of phenol over delaminated Fe-Ti-PILC employing microwave irradiation. Catal. Commun. 5, 437–440.

Mojović, Z., Banković, P., Milutinović-Nikolić, A., Dostanić, J., Jović-Jovičić, N., Jovanović, D., 2009. Al, Cu-pillared clays as catalysts in environmental protection. Chem. Eng. J. 154, 149–155.

Molina, C.B., Zazo, J.A., Casas, J.A., Rodriguez, J.J., 2010. CWPO of 4-CP and industrial wastewater with Al-Fe pillared clays. Water Sci. Technol. 61, 2161–2168.

Nogueira, R.F.P., Oliveira, M.C., Paterlini, W.C., 2005. Simple and fast spectrophotometric determination of H_2O_2 in photo-Fenton reactions using metavanadate. Talanta 66, 86–91.

Park, C., Baker, R.T.K., 2002. Modifications in the catalytic properties of nickel supported on different dielectric oxides. Chem. Mater. 14, 273–280.

Perathoner, S., Centi, G., 2005. Wet hydrogen peroxide catalytic oxidation (WHPCO) of organic waste in agro-food and industrial steams. Top. Catal. 33, 207–224.

Pera-Titus, M., Garćia-Molina, V., Baños, M.A., Giménez, J., Esplugas, S., 2004. Degradation of chlorophenols by means of advanced oxidation processes: A general review. Appl. Catal. B Environ. 47, 219–256.

Quintanilla, A., Casas, J.A., Rodriguez, J.J., 2010. Hydrogen peroxide-promoted-CWAO of phenol with activated carbon. Appl. Catal. B Environ. 93, 339–345.

Robert, R., Barbati, S., Ricq, N., Ambrosio, M., 2002. Intermediates in wet oxidation of cellulose: Identification of hydroxyl radical and characterization of hydrogen peroxide. Water Res. 36, 4821–4829.

Rokhina, E.V., Virkutyte, J., 2011. Environmental application of catalytic processes: Heterogeneous liquid phase oxidation of phenol with hydrogen peroxide. Crit. Rev. Environ. Sci. Technol. 41, 125–167.

Sanabria, N.R., Ávila, P., Yates, M., Rasmussen, S.B., Molina, R., Moreno, S., 2010. Mechanical and textural properties of extruded materials manufactured with AlFe and AlCeFe pillared bentonites. Appl. Clay Sci. 47, 283–289.

Silva, A.M.T., Herney-Ramirez, J., Söylemez, U., Madeira, L.M., 2012. A lumped kinetic model based on the Fermi's equation applied to the catalytic wet hydrogen peroxide oxidation of acid orange 7. Appl. Catal. B Environ. 121–122, 10–19.

Tatibouët, J.M., Guélou, E., Fournier, J., 2005. Catalytic oxidation of phenol by hydrogen peroxide over a pillared clay containing iron. Active species and pH effect. Top. Catal. 33, 225–232.

Timofeeva, M.N., Khankhasaeva, S.T., Badmaeva, S.V., Chuvilin, A.L., Burgina, E.B., Ayupov, A.B.., Panchenko, V.N., Kulikova, A.V., 2005. Synthesis, characterization and catalytic application for wet oxidation of phenol of iron-containing clays. Appl. Catal. B Environ. 59, 243–248.

Velegraki, T., Nouli, E., Katsoni, A., Yentekakis, I.V., Mantzavinos, D., 2011. Wet oxidation of benzoic acid catalyzed by cupric ions: Key parameters affecting induction period and conversion. Appl. Catal. B Environ. 101, 479–485.

Vicente, M.A., Bañares-Muñoz, M.A., Gandía, L.M., Gil, A., 2001. On the structural changes of a saponite intercalated with various polycations upon thermal treatments. Appl. Catal. A Gen. 217, 191–204.

Wang, S.W., Dong, Y.H., He, M.L., Chen, L., Yu, X.J., 2009. Characterization of GMZ bentonite and its application in the adsorption of Pb(II) from aqueous solutions. Appl. Clay Sci. 43, 164–171.

Yuan, P., Annabi-Bergaya, F., Tao, Q., Fan, M.D., Liu, Z.W., Zhu, J.X., He, H.P., Chen, T.H., 2008. A combined study by XRD, FTIR, TG and HRTEM on the structure of delaminated Fe-intercalated/pillared clay. J. Colloid Interface Sci. 324, 142–149.

Zhou, S.W., Gu, C.T., Qian, Z.Y., Xu, J.G., Xia, C.H., 2011a. The activity and selectivity of catalytic peroxide oxidation of chlorophenols over Cu-Al hydrotalcite/clay composite. J. Colloid Interface Sci. 357, 447–452.

Zhou, S.W., Qian, Z.Y., Sun, T., Xu, J.G., Xia, C.H., 2011b. Catalytic wet peroxide oxidation of phenol over Cu-Ni-Al hydrotalcite. Appl. Clay Sci. 53, 627–633.

Zrnčević, S., Gomzi, Z., 2005. CWPO: An environmental solution for pollutant removal from wastewater. Ind. Eng. Chem. Res. 44, 6110–6114.